High Vibrational State Energy Redistribution in Two Deuterated Cyclopentenes

L. Lespade* and D. Cavagnat

Laboratoire de Physico-Chimie Moléculaire, UMR 5308, Université de Bordeaux I, 33405 Talence Cedex, France

S. Rodin-Bercion

Laboratoire COVACHIM, EA 925 Université des Antilles et de la Guyane, BP 250, 97157 Pointe à Pitre Cedex, France

Received: May 11, 2000; In Final Form: August 3, 2000

The high CH bond stretching vibrational states spectra (from $\Delta v = 1$ to 6) are presented for two isotopomers of cyclopentene: cyclopentene-1,2,3,4,4,5,5-d_7 and cyclopentene-4,4,5,5-d_4. They are analyzed simultaneously with a model Hamiltonian expressed in internal curvilinear coordinates. Because of the size of the molecules, only the CH_2 or CHD chromophore is considered in the calculations (two bond stretches and five angle deformations). The results show a reasonable agreement between the experimental and calculated spectra for the two molecules with the use of the same anharmonic potential.

I. Introduction

The study of intramolecular vibrational energy redistribution (IVR) has drawn the attention of scientists for a long time because it may give detailed insight into molecular energy states before photodissociation or laser-induced reaction.[1−3] Many of the experimental investigations in the field of intramolecular dynamics have been performed in the frequency domain. On the short time scale, IVR has been shown to be largely uncorrelated to the total state density [4,5] but to be ruled by strong couplings with specific states. Moreover, anharmonic short time resonance dynamics seems to be characteristic for certain functional groups[2] and transferable between different molecules containing the same functional groups. The present work is situated in the frame of IVR studies of the methylenic group. The vibrational energy flow characteristic of this functional group has been studied in cyclic molecules such as cyclohexene[6] or monohydrogenated cyclopentene.[7,8] But the overtone spectra have been modeled in normal coordinates and thus, the anharmonic potentials describing the energy flow were not transferable from one molecule to another. In the present study, we have focused our attention on the intramolecular vibrational energy redistribution in the overtone region of CH stretches of two isopotomers of the cyclopentene molecule, one with one CHD methylene group, the cyclopentene-1,2,3,4,4,5,5-d_7 ($3h_1$) molecule and one with a CH_2 group on the same carbon, cyclopentene-4,4,5,5-d_4 (d_4) (Figure 1). The vibrational energy flow has been modeled simultaneously for the two molecules with the assumption that the doorway states which rule the vibrational energy flow are linked to the methylene chromophore. That is to say, the doorway states are combinations involving the deformations of the five angles attached to the functional group. In a first step, the combinations involving the CC stretches are disregarded because they are completely delocalized along the cyclopentene ring. The results of the calculations will demonstrate to what extent and for which wavenumber region this approximation is correct and the CH stretching overtones are coupled to the ring stretches.

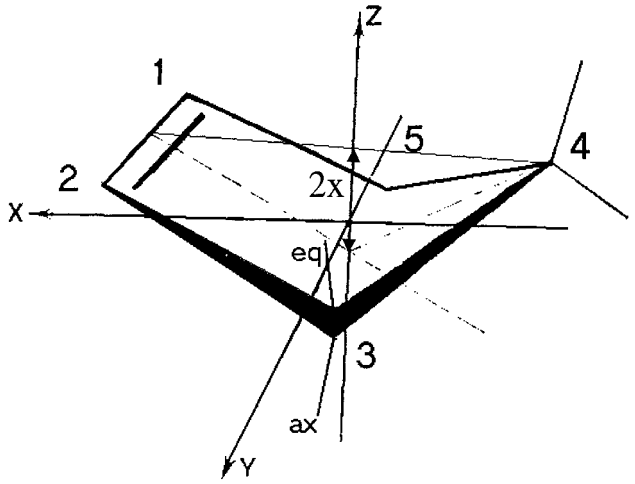

Figure 1. Definition of the ring-puckering coordinate x when the molecule is in its bent equilibrium conformation.

In flexible molecules, the CH stretching vibrations are coupled to large amplitude motion.[9] When the motion is slow enough with respect to the vibrational energy redistribution, as is the case in cyclopentene molecules, the coupling between the vibrations and the large amplitude motion can be treated in the adiabatic approximation. Indeed, the ring-puckering period is of the order of a few picoseconds[10] which is much slower than the rapid energy flow in cyclopentene. When there are strong Fermi resonances, the characteristic time of the energy flow has been estimated to be less than 100 fs. The adiabatic approximation has proved powerful in describing the high vibrational states of nitromethane[12,13] or cyclopentene.[7−8] In particular, it clears up the discrepancy between the spectra of the first CH stretching excited states of different isotopomers of the same molecule. Indeed, the coupling between the two motions can be described by an effective potential that contains a vibrational part corresponding to the variation of vibrational energy during internal motion.[7,12,13] For the monohydrogenated molecule, that vibrational energy breaks the symmetry of the

10.1021/jp001743+ CCC: $19.00
Published on Web 10/19/2000

effective potential modifying the large amplitude motion levels of the vibrationally excited molecule. As a consequence, the spectra, which are the sum of all the transitions between the two effective potentials corresponding to the ground state and the vibrationally excited molecule, show an extra band constituted of all the transitions issued from large amplitude motion levels above the potential barrier. In the monohydrogenated nitromethane molecule $\Delta v = 1$ spectrum,[12] this component is the more important of the spectrum and is situated at 15 cm^{-1} above the transition issued from the fundamental level. In monohydrogenated cyclopentene molecules, the transitions issued from ring-puckering levels above the potential barrier are situated at wavenumbers intermediate between the axial and the equatorial ones.[10] Their intensities are less important than is the case for the nitromethane molecule because the potential has a higher barrier. For hydrogenated molecules, when the coupling between the CH stretches is effective (normal mode regime), the vibrational energy flows from one CH bond to another in order to minimize its variation during the motion.[13] Thus, the excited-state potential is not very different from the fundamental potential and keeps the same symmetry. As a consequence, all the transitions between the two potentials have almost the same wavenumbers. The best example is the symmetric CH stretching band of perhydrogenated nitromethane.[13] The vibrational variation of that normal mode is very weak (0.5 $\cos(6\theta)$ in cm^{-1}). Thus, the two effective potentials are very similar and all the transitions are at the same position, giving rise to only one band at the resolution of the spectrum. However, for the higher overtones, the localization of the vibrational energy may induce, even in fully hydrogenated molecules, an asymmetry of the excited effective ring-puckering potential as in monohydrogenated molecules. This explains why the high energy state spectra of different isotopomers may be similar if they are not too much perturbed by Fermi resonances.

These phenomena will be illustrated in the study of the overtone spectra of the two cyclopentene molecules ($3h_1$ and d_4). The structure of the present paper will be as follows: after presentation of the experimental details, the theoretical basis for the modeling of the spectra will be presented. The experimental spectra are then discussed in view of the modeled spectra of the two compounds.

II. Experiment

Cyclopentene-4,4,5,5-d_4 (cyclopentene-d_4) was purchased at MSD and monohydrogenated cyclopentene (cyclopentene-$3h_1$) was synthesized by the organic route according to the procedure described in ref 14. The products were dried with sodium filaments, degassed by the freeze pump thaw method, and transferred under vacuum into the cells.

The near-infrared spectra ($\Delta v = 1-4$) were recorded by standard absorption spectroscopy on a Nicolet 740 FTIR spectrometer (resolution 1 cm^{-1}) between 2700 and 8600 cm^{-1} and a BioRad FTS-60A spectrometer (resolution 2 cm^{-1}) between 8600 and 11 500 cm^{-1}. An Infrared Analysis long path minicell equipped with CaF_2 windows ($l = 1-7.2$ m) was used.

The visible spectra ($\Delta v = 5,6$) were recorded with the intracavity photoacoustic spectrometer which has been described elsewhere.[15] The pump laser is a 4 W Ar ion laser (Coherent Innova 70), chopped at 85 Hz. The photoacoustic cell is placed inside the cavity of a linear Coherent 599 dye laser. The spectral line width is 0.7 cm^{-1}, and the absolute wavelengths are measured with a Raman PH0 spectrometer to within ± 2 cm^{-1}. We have used the following dyes: Pyridine 2 for the fourth overtone and DCM for the fifth. Each spectrum was measured with a vapor pressure of 200 Torr.

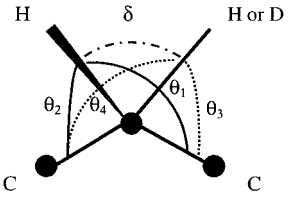

Figure 2. Definition of the methylene chromophore angle coordinates.

III. Theoretical Approach

The theoretical approach in the analysis of the spectra has previously been described in the first papers on cyclopentene.[7,8] The difference in the present work resides in the writing of the vibrational Hamiltonian. The previous Hamiltonian was expressed in curvilinear normal coordinates. With the use of these coordinates, the anharmonic potential terms cannot be transferred from one molecule to another because they are characteristic of the normal modes of the molecule. In this work, curvilinear internal coordinates are preferred because they allow a simultaneous fit of different isotopomers of the same molecule with different symmetry. The simultaneous fit of the spectra of different isotopomers can be done in symmetry coordinates[16] when the compounds have the same symmetry. But when the symmetry is broken by deuteration, only internal coordinates can be employed. This has the disadvantage of increasing the degrees of freedom, and thus the size of the basis states. In the cyclopentene molecule, if one supposes that the doorway states ruling the vibrational energy flow are linked to the methylene chromophore, one has to consider the nine internal coordinates attached to the CH_2 group: the two CH or CD stretches, five angle deformations (because of the redundancy) and the two CC stretches. The two CC stretches are strongly coupled to the remaining part of the molecule giving rise to many ring modes which are generally also coupled to the other vibrations.[17] Thus, even if combinations of CC stretching and angle deformation are anharmonically coupled to the CH stretches through the kinetic matrix, these couplings are very diluted inside bath modes and can be neglected in a first step. As a consequence, the high vibrational states of the two cyclopentene molecules, $3h_1$ and d_4, will be modeled by a vibrational Hamiltonian H_{v-r} describing the vibrations of the seven curvilinear internal coordinates: the two CH or CD stretches and the five angle deformations attached to the methylene (Figure 2).

The total Hamiltonian is the sum of the vibrational Hamiltonian $H_{v-r}(q,x)$, which will be developed below, and of a ring-puckering Hamiltonian $H_r(x)$:

$$H_T(x,q) = H_{v-r}(q,x) + H_r(x) \tag{1}$$

The ring-puckering Hamiltonian used for the description of the large amplitude motion is well-known:[14,17,18]

$$\frac{H_r(x)}{hc} = -\frac{\hbar^2}{2hc}\left(\frac{\partial}{\partial x}\right)g(x)\left(\frac{\partial}{\partial x}\right) + V(x) \tag{2}$$

In this expression, $g(x)$ is the inverse of the reduced mass of the motion and $V(x)$ the potential function. $g(x)$ is calculated by using the basis bisector model of Malloy[19] where the motions of the ring atoms are assumed to be curvilinear and the HCH angle bisectors are constrained to be collinear with the CCC angle bisectors. A more elaborate model does not lead to any real improvement of the fit of the far-infrared spectrum.[17]

TABLE 1: Ground State Ring-Puckering Potentials of the Two Compounds (from Refs 14 and 18)[a]

Cyclopentene-3h$_1$	$V_{\text{eff}}(0,x) = -26\,452\,x^2 + 952\,x^3 + 754\,020\,x^4$
Cyclopentene-d_4	$V_{\text{eff}}(0,x) = -24\,959\,x^2 + 000\,x^3 + 696\,164\,x^4$

[a] The potentials are expressed in cm^{-1} and x in Å.

The coupling between the large amplitude ring-puckering motion and the vibrations is solved in the adiabatic approximation: the total wave function can be separated into two wave functions, one for the ring-puckering motion, $\psi(x)$ and one for the molecular vibrations $\varphi(x,q)$.

As a consequence, the Schrödinger equation solving the total Hamiltonian can be separated into two equations. The first models the fast vibrations for every position of the molecule during large amplitude motion. In the second, the ring-puckering potential is increased by the vibrational energy $e(x)$, obtained by solving the vibrational equation.

For the $(\upsilon - 1)$ overtone, the reconstruction of the vibrational spectra are completed in two steps. The diagonalization of the vibrational Hamiltonian matrix for each x position gives the vibrational energy $e_n(x) = hc\ \omega_n(\upsilon,x)$:

$$\sum_i \mathrm{H}^{ij}_{\upsilon-r}(\upsilon, x)c_{in}(\upsilon, x) = hc\omega_n(\upsilon, x)c_{jn}(\upsilon, x) \qquad (3)$$

where the c_{jn} (υ,x) are the eigenvector elements corresponding to the wave functions of the combinations of vibrations of the seven internal coordinates attached to the CH_2 chromophore (the two CH or CD stretches and the five angles).

The vibrational energy $e_n(x)$ is then added to the fundamental state ring-puckering effective potential $V_{\text{eff}}(0,x)$ to form the excited-state ring-puckering effective potential.

$$V^n_{\text{eff}}(\upsilon, x) = hc\omega_n(\upsilon, x) + V_{\text{eff}}(0, x) \qquad (4)$$

It should be stressed that $V_{\text{eff}}(0,x)$ is different from $V(x)$ since it is the sum of $V(x)$ and of the zero point vibrational energy $\omega(0,x)$.[17] The fundamental state ring-puckering effective potential $V_{\text{eff}}(0,x)$ can be obtained for the two compounds by fitting the far-infrared transitions.[14,18] They generally are fitted by a fourth order polynomial form as a function of x, the ring-puckering coordinate (Table 1). It should be noted that the cyclopentene-d_4 potential has only even power terms because the molecule has a C_s symmetry in the plane conformation.

The spectra are made up of all the transitions between the potential $V_{\text{eff}}(0,x)$ and the excited-state potentials $V^n_{\text{eff}}(\upsilon,x)$ corresponding to the vibrational energies $e_n(x)$ the eigenvectors of which have a nonnegligible component of pure CH bond stretching. These transitions are calculated as explained in ref 16.

Inside each polyad, the mode intensities are supposed to come from the CH bond stretching overtones only. They depend on the quantity $\langle 0|\mu(x)|V_n\rangle$ where $\mu(x)$ is the molecular dipole moment and $|V_n\rangle$ the eigenstate of wavenumber $hc\omega_n$ corresponding to stretching quantum numbers equal to the considered polyad υ:

$$|V_n\rangle = \sum_{i=1}^{2} c_{\text{in}}|\upsilon_{r_i} = \upsilon,\ \upsilon_{r_{j\neq i}} = 0,\ \upsilon_\delta = 0,\ \upsilon_{w_j} = 0\rangle$$

υ_δ is the quantum number in HCH bending coordinate and υ_{wj} are the quantum numbers in the four HCC deformations. The dipole moment function can be developed as a Taylor series expansion in the internal stretching displacement coordinates r_i around the equilibrium geometry. It is a function of the dipole moment derivatives $\mu_{ni}{}^j(x)$:

TABLE 2: Components of the First Dipole Moment Derivatives (Debye/Å) as Calculated from the Atomic Polar Tensor Given by the Ab Initio Calculations

C−H bond		$\partial\mu^x/\partial r$	$\partial\mu^y/\partial r$	$\partial\mu^z/\partial r$	$\|\|\partial\bar{\mu}/\partial r\|\|$
α	C_3H_9 (ax)	0.038 05	0.163 08	0.213 15	0.271
	C_3H_8 (eq)	0.0552	0.227 91	−0.127 13	0.2667
in plane position		0.043 34	0.201 68	0.182 19	0.275

$$\mu^j_{ni}(x) = \frac{\delta^n \mu_j(x)}{\delta r_i^{\,n}} \qquad (5)$$

where $\mu_j(x)$ is the jth component ($j = x,y,z$) of the dipole moment and r_i is the ith CH bond stretching displacement coordinate. Such quantities can be obtained from a dipole moment surface[12] but are not available for the cyclopentene molecule. However, the first moment derivatives $\mu^j_{1i}(x)$ ($j = x,y,z$) can be derived from the atomic polar tensors introduced by Biarge, Herranz, and Morcillo[20] and reformulated by Person and Newton[21] which are available from ab initio calculations. The first moment derivatives derived from the ab initio calculation atomic polar tensor are given in Table 2. They have been obtained with a Gaussian 92 calculation[22] using a 6-31G** basis set. In the bent conformation, the first derivative of the dipole moment is slightly tilted from the CH bond by 12° for the equatorial bond and by 14° for the axial bond. Its magnitude differs by less than 2% for the two conformations. This first-order term is dominant for the $\Delta\upsilon = 1$ spectrum. Thus the infrared intensity of the CH stretching transitions between two states, $|0,k'\rangle \rightarrow |1,k\rangle$ ($|0,k'\rangle$ and $|1,k\rangle$ being, respectively, the k'th and kth ring-puckering levels in the ground and first excited vibrational states corresponding to $\omega_n(x)$ is given by:

$$I^n_{|1,k\rangle\leftarrow|0,k'\rangle} = \nu_{1k,0k'} P \sum_i^2 \left(\int \psi^*_{1k}(x)\langle 0|\bar{\mu}_{1i}(x) r_i|\upsilon\rangle c_{in}(x)\psi_{0k'}(x)\mathrm{d}x\right)^2 \qquad (6)$$

where P is the Boltzmann factor, $\exp[-(E_{0k} - E_{00})/kT]$, ψ_{1k} and $\psi_{0k'}$ the ring-puckering wave functions of the $|1,k\rangle$ and $|0,k'\rangle$ states and $\bar{\mu}_{1i}$ is the vector of components $\mu_{1i}{}^j(x)(j = x,y,z)$. In the monohydrogenated molecule, there is no summation on i.

For the overtone spectra, the higher order terms of the dipole moment expansion also have an important contribution in the transition intensities. Since these higher derivatives are not available, one can suppose with a good approximation that the quantity $\langle 0|\bar{\mu}(x)|V_n\rangle$ is the sum of the two quantities $\langle 0|\bar{\mu}_i(x)|\upsilon\rangle$, each of them being collinear to the ith CH bond. Only their dependence on x is needed since the absolute intensity is not calculated.[17] The infrared intensity of the CH stretching transitions between two states, $|0,k'\rangle \rightarrow |\upsilon,k\rangle$, is then given by:

$$I^n_{|\upsilon,k\rangle\leftarrow|0,k'\rangle} = \nu_{\upsilon k,0k'} P \sum_i^2 \left(\int \psi^*_{\upsilon k}(x)\langle 0|\bar{\mu}_i(x)|\upsilon\rangle c_{in}(x)\psi_{0k'}(x)\mathrm{d}x\right)^2 \qquad (7)$$

where P is the Boltzmann factor, $\exp[-(E_{0k} - E_{00})/kT]$. In the monohydrogenated molecule, there is no summation on i. The bond dipole approximation seems reasonable in that sort of cyclic molecule since some calculations performed on cyclohexane[23] show that the intensity ratio between the two axial or equatorial transition intensities is not strongly modified from

one overtone to another. In cyclopentene, the conformational dependence of the magnitude of the dipole moment is very weak at $\Delta v = 1$. Thus, the assumption of no conformational dependence in the overtones is within the uncertainty of our calculations. For local modes, the direction of the dipole moment is essentially important in the reproduction of the band shapes. A breakdown of the bond dipole moment approximation would lead to a bad reproduction of the spectrum profiles.

The Vibrational Hamiltonian. The quantum mechanical Hamiltonian in curvilinear internal coordinates is:[24]

$$H_{v-r} = T + V = -\frac{1}{2}\hbar^2 g^{1/4}\sum_{ij}\frac{\partial}{\partial q_i}g^{-1/2}g_{ij}\frac{\partial}{\partial q_j}g^{1/4} + V(q) \quad (8)$$

where g_{ij} are the Wilson matrix elements and $g = \det|g_{ij}|$.

The kinetic part can also be expressed in a more simple expression:[25]

$$T = \frac{1}{2}\sum_{i,j} p_i g_{ij}(q) p_j + V'(q) \quad (9)$$

where V' is the mass dependent potential-like kinetic term. This term is small[26] in heavy molecules such as cyclopentene and is neglected. For methane, Wang and Sibert[26] have shown that V' first contributes to the perturbative calculation of the transition wavenumbers at the third order. In the present work, the first term of the quantum mechanical vibrational Hamiltonian is only developed up to the second order[27] since, because of the size of the molecule, other approximations are made (in particular the neglect of the CC stretching couplings).

At zero order, the CH or CD stretchings are described by Morse oscillators and the angles by anharmonic oscillators:

$$\frac{H^0_{v-r}}{hc} = \frac{1}{2}\sum_{i}^{2}\{g^0_{r_ir_i}p_{r_i}p_{r_i} + D_i(x)[1 - e^{-a_i(x)r_i}]^2\} + \sum_{i=j}\left\{\frac{1}{2}g^0_{r_ir_j}p_{r_i}p_{r_j} + \frac{1}{2}f_{rr'}(x)r_ir_j\right\} + \sum_{i}^{5}\sum_{j}^{5}\left\{\frac{1}{2}(g^0_{\alpha_i\alpha_j}p_{\alpha_i}p_{\alpha_j} + f_{\alpha_i\alpha_j}(x)\alpha_i\alpha_j + f_{\alpha_i\alpha_i\alpha_i}(x)\alpha_i^3 + f_{\alpha_i\alpha_i\alpha_i\alpha_i}(x)\alpha_i^4)\right\} \quad (10)$$

In this expression, the r_i variables are the CH or CD bond displacement coordinates and α_i are the valence angle displacement coordinates (α_1 is HCH or HCD, α_2 and α_3 are the HCC angle deformations adjacent to the first bond r_1, and α_4 and α_5 are the HCC angle deformations adjacent to r_2)(see Figure 2). The kinetic terms of the G matrix depend only on the geometry of the methylene chromophore. The ab initio calculations indicate a small variation of the angles during the large amplitude motion. In this study, this variation has been disregarded since it leads to G matrix element changes of less than two percent. All the angles have been kept to their tetrahedral value of 109°. $D_i(x)$ is the dissociation energy of the ith CH bond and $a_i(x)$ the Morse potential parameter. They are related to the harmonic wavenumber $\omega_{0i}(x)$ and the anharmonicity $\chi_i(x)$.[28] Their dependence on the ring-puckering coordinate is directly linked to the variation of $\omega_{0i}(x)$ which can be evaluated from the ab initio calculations.[17]

The first order expansion of the vibrational Hamiltonian gives the anharmonic couplings involved in the Fermi resonances between the CH overtones and combination states. Only the most important terms of the kinetics energy are retained. They correspond to the Taylor series expansion of the Wilson g matrix elements $g_{\alpha\alpha}$ and $g_{r\alpha}$ in the displacement or deformation coordinates about the equilibrium configuration.[29]

$$\frac{H^1_{v-r}}{hc} = \frac{1}{2}\sum_{i=1}^{2}\sum_{j=1}^{5}\left\{\left(\frac{\partial g^0_{\alpha_j\alpha_j}}{\partial r_i}\right)_e r_i p^2_{\alpha_j} + \left(\frac{\partial g^0_{r_i\alpha_j}}{\partial \alpha_j}\right)_e p_{r_i}p_{\alpha_j}\alpha_j + \sum_{k=1}^{5}\left[\left(\frac{\partial g^0_{\alpha_j\alpha_k}}{\partial r_i}\right)_e p_{\alpha_j}p_{\alpha_k}r_i + \left(\frac{\partial g^0_{r_i\alpha_j}}{\partial \alpha_k}\right)_e p_{r_i}p_{\alpha_j}\alpha_k\right]\right\} + \frac{1}{2}\sum_{i=1}^{2}\sum_{j=1}^{5}\sum_{k=1}^{5}\{f_{r_i\alpha_j\alpha_k}(x)r_i\alpha_j\alpha_k\} \quad (11)$$

The most important terms in the kinetic matrix development are the $(\partial g^0_{\alpha_j\alpha_j}/\partial r_i)_e$ and $(\partial g^0_{\alpha_j\alpha_k}/\partial r_i)_e$ terms where the bond corresponding to r_i is adjacent to the angles α_j and α_k. Thus, the combination states which are the most kinetically coupled to the CH stretching are the overtone of the HCH or HCD deformation and of the HCC angle deformations adjacent to the considered CH bond and combination states of these three angle deformations. The other terms, although smaller, have a nonnegligible importance in the IVR.

The relevant terms in the second order expansion are less numerous since only the squares of the deformation coordinates give rise to diagonal contributions.

$$\frac{H^2_{v-r}}{hc} = \frac{1}{4}\sum_{i=1}^{2}\sum_{j=1}^{5}\left\{\left(\frac{\partial^2 g^0_{\alpha_j\alpha_j}}{\partial r_i^2}\right)_e r_i^2 p^2_{\alpha_j} + f_{r_ir_i\alpha_j\alpha_j}(x)r_i^2\alpha_j^2\right\} \quad (12)$$

Modeling of the Spectra. The effective vibrational Hamiltonian is represented in a basis set whose functions are products of Morse oscillator functions for CH or CD bond stretches and harmonic oscillator wave functions for bending modes. The matrix elements are calculated for all the basis functions that are the product of the seven wave functions of all the possible combinations of the seven coordinate vibrations corresponding to a given overtone. The zero order Hamiltonian (eq 10) gives the unperturbed energy for the state $|v\rangle = |v_{r_i}, v_\delta, v_{w_j}\rangle$ where $\delta = \alpha_1$ and $w_j = \alpha_{j+1}$:

$$E(x, v) = \sum_{i=1}^{2}\left(\omega_{0i}(x)\left(v_{r_i} + \frac{1}{2}\right) - \chi_i(x)\left(v_{r_i} + \frac{1}{2}\right)^2\right) + \omega_\delta(x)\left(\nu_\delta + \frac{1}{2}\right) - \chi_\delta(x)\left(v_\delta + \frac{1}{2}\right)^2 + \sum_{k=1}^{4}\left(\omega_{w_k}(x)\left(v_{w_k} + \frac{1}{2}\right) - \chi_{w_k}(x)\left(v_{w_k} + \frac{1}{2}\right)^2\right) \quad (13)$$

where ω_δ stands for the bending harmonic wavenumber, and χ_δ its anharmonicity, ω_{wj} is the harmonic wavenumber of the jth HCC deformation (Figure 2) and χ_{wj} its anharmonicity. The expansion of the first-order Hamiltonian on the basis set gives the Fermi resonance couplings, and the first and second-order Hamiltonian expansion the cross anharmonicities.[7]

Then, the vibrational Hamiltonian matrix is solved for every x value between −0.30 and 0.30 Å with a step of 0.01 Å. The result of the diagonalization gives the vibrational variations $hc\omega_n(x)$ and the corresponding eigenvector elements $c_{ni}(x)$ (i = 1 or 1,2) of pure CH stretch overtone. The energies are fitted by a least-squares method to a sixth-order polynomial form and the eigenvectors to a ninth-order one. The transitions between the effective potentials $V_{\text{eff}}(0,x)$ and $V^n_{\text{eff}}(v,x)$ are then calculated as described previously and added to form the

TABLE 3: Effective Parameters Used in the Modeling of the Spectra (x Is in Å)

local parameters for the CH(CD) bond stretching modes (cm^{-1})		
$\omega_0(x) = (3044.5 + 268x - 439x^2 - 4300x^3 + 11\,000x^4)$	for the CH stretches	
$\omega_0(x) = (3044.5 + 268x - 439x^2 - 4300x^3 + 11\,000x^4)/\sqrt{1.857}$	for the CD stretches	
$\chi\,(x) = 64.6 - 2.5x - 34.5x^2 - 44.5x^3 + 1250x^4$	for the CH stretches	
$\chi\,(x) = 32.6 + (-2.5x - 34.5x^2 - 44.5x^3 + 1250x^4)/\sqrt{2}$	for the CD stretches	
The $a(x)$ and $D(x)$ can be readily obtained from these parameters (ref 27)		
$f_{rr'} = 0.055 + 1.042\,x^2$ (in mdyn/Å)		
Parameters for the bends in cm^{-1} (δ labels the HCH or HCD deformation and w_i the HCC bends; $i = 1,4$; see Figure 2):		
$\omega_\delta(x) = (1306 - 250x^2 + 4000x^4)$	for the HCH bend[a]	
$\chi_\delta(x) = 8$		
$f_{r\delta\delta}(x) = -0.28 + 0.17x + 5.55x^2$ (in mdyn)		
$f_{rr\delta\delta}(x) = 5.55$ (in mdyn/Å)		
$\omega_{w_i}(x) = (1125 + 52x - 150x^2 + 4000x^4)$	$i = 1,2$ for the HCC deformation[a]	
$\omega_{w_i}(x) = (1125 - 52x - 150x^2 + 4000x^4)$	$i = 3,4$	
$\chi_{w_i}(x) = 9 + 8x$	$i = 1,2$	
$\chi_{w_i}(x) = 9 - 8x$	$i = 3,4$	
$f_{r_1w_1w_1} = f_{r_1w_2w_2} = -0.545 - 0.21x$	$f_{r_2w_3w_3} = f_{r_2w_4w_4} = -0.545 + 0.21x$	(in mdyn)
$f_{r_1w_3w_3} = f_{r_1w_4w_4} = -0.82x$	$f_{r_2w_1w_1} = f_{r_2w_2w_2} = 0.82x$	(in mdyn)
$f_{r_1\delta w_1} = f_{r_1\delta w_2} = 0.385 + 0.3x$	$f_{r_2\delta w_3} = f_{r_2\delta w_4} = 0.385 - 0.3x$	(in mdyn)
$f_{r_1\delta w_3} = f_{r_1\delta w_4} = -0.15 - 0.4x$	$f_{r_2\delta w_1} = f_{r_2\delta w_2} = -0.15 + 0.4x$	(in mdyn)
$f_{r_1w_1w_2} = -0.82 - 0.45x$	$f_{r_2w_3w_4} = -0.82 + 0.45x$	(in mdyn)
$f_{r_1w_1w_3} = f_{r_1w_2w_4} = 0$	$f_{r_2w_1w_3} = f_{r_2w_2w_4} = 0$	(in mdyn)
$f_{r_1r_1w_1w_1} = f_{r_1r_1w_2w_2} = 0.9 + 0.03x$	$f_{r_2r_2w_3w_3} = f_{r_2r_2w_4w_4} = 0.9 - 0.03x$	(in mdyn/Å)

The effective interaction matrix between the angle deformations $f_{\alpha_i\alpha_j}$ (in mdynÅ)

	δ	w_1	w_2	w_3	w_4
δ	—	0.04	0.04	0.04	0.04
w_1	0.04	—	0.141	0.02	0.04
w_2	0.04	0.141	—	0.04	0.02
w_3	0.04	0.02	0.04	—	0.141
w_4	0.04	0.04	0.02	0.141	—

[a] The parameters of the deuterated angle deformations are readily obtained by dividing the nondeuterated ones by the square root of the ratio of the G matrix elements corresponding to deuterated and undeuterated angle deformations.

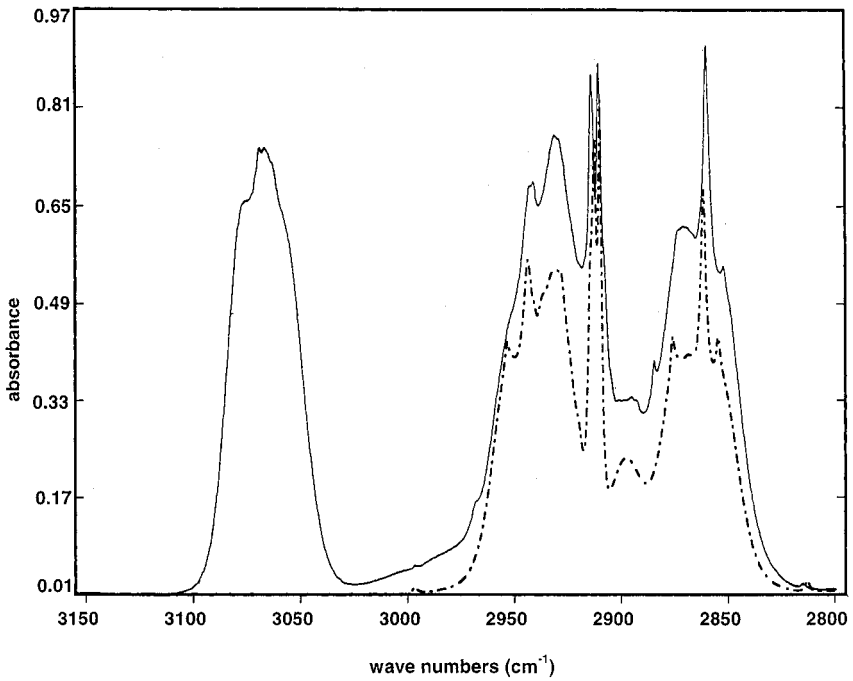

Figure 3. Observed and calculated spectra of the first excited CH bond stretching in cyclopentene-d_4. The observed spectrum (top solid line) was obtained by FTIR with a 10 cm path length cell and a pressure of 30 Torr. The dashed line represents the calculated spectrum with a vibration−rotation theoretical profile which has been convoluted by a 2 cm^{-1} half-width Lorentzian band (fwhh). (See text.)

spectrum of the ($v - 1$) overtone. The effect of the rotation of the entire molecule is taken into account by convoluting each transition by the theoretical asymmetrical top vibration−rotation profile corresponding to each component of the dipole moment along the molecular principal axes determined by ab initio calculations (A, B, C type, depending on whether the transition considered involves the μ_x, μ_y or μ_z dipole moment component).[30] The B type has only a PR profile with no Q branch and the C type has a sharp Q branch. To model the broadening of the bands when the energy increases, this profile is convoluted

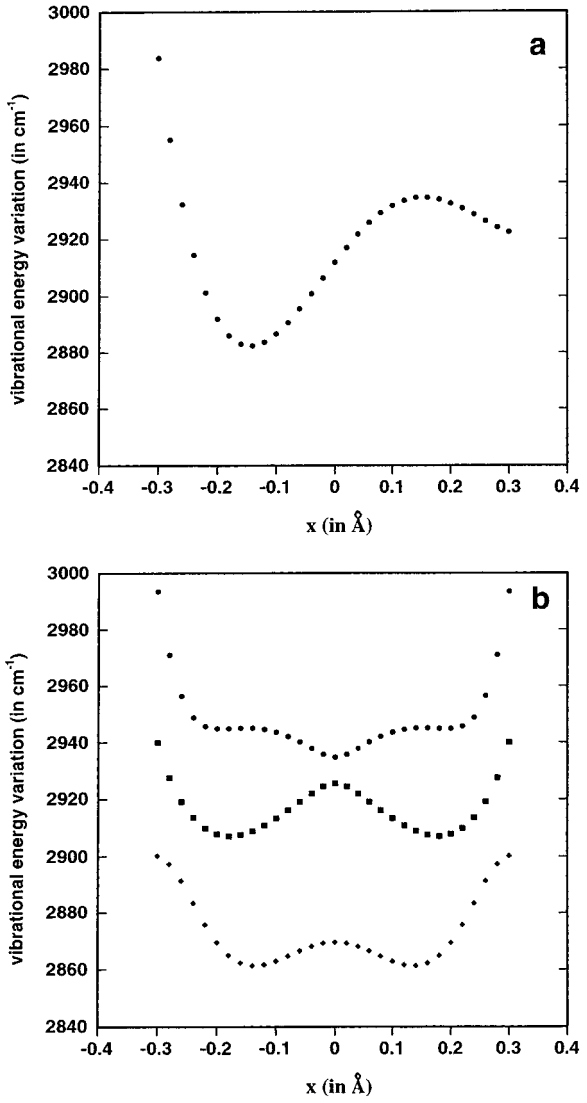

Figure 4. Calculated vibrational energy variations for cyclopentene-$3h_1$ (a) and cyclopentene-d_4 (b) at $\Delta v = 1$. The axial bent conformation corresponds to a value of $x = -0.13$ Å and the equatorial bent conformation to $x = 0.13$ Å. The ring-puckering wave functions corresponding to the levels above the potential barrier are generally delocalized but the first ones are centered at $x = 0$ Å (plane conformation).

by a Lorentzian shape with a half-width adapted to the experimental overtone spectrum.

IV. Discussion

In the modeling of the overtone spectra, all the parameters displayed in Table 3 have been adjusted in order to reproduce both the experimental wavenumbers and the transition intensities of the two compounds.

1. First Excited Spectra. The first excited-state spectrum of cyclopentene-d_4 is displayed in Figure 3. It has to be compared with that of cyclopentene-$3h_1$ published in ref 17. When there is no Fermi resonance, the CH stretching spectrum of the monohydrogenated compound depends essentially on the variation of the CH stretching wavenumber during the motion. This variation can be evaluated from the ab initio calculation[17] (Figure 4a). But the anharmonic couplings, which are not taken into account in ref 17, slightly modify the harmonic CH stretching wavenumbers. It is for this reason that the local parameters for the CH bond stretching modes listed in Table 3 are slightly different from those listed in ref 17. The calculated spectrum is absolutely equivalent to that published in ref 17. It is composed of essentially three main absorptions corresponding to the transitions issued from the two ring-puckering levels in the potential wells and from levels above the barrier. The spectrum of the cyclopentene-d_4 compound is very different (Figure 3). The calculated variation of the vibrational energy can explain this discrepancy (Figure 4). Because of the coupling between the two CH bond stretches, the vibrational energy flows from one bond to the other minimizing its variation during the motion (typically between -0.13 Å for one bent conformation to 0.13 Å for the other). The effective potentials of the excited state remain symmetric and are not very different from the ground effective potential. As a consequence, the transitions issued from the levels above the ring-puckering barrier have wavenumbers very similar to that of the transitions issued from the levels inside the potential well. Apart from the 3070 cm^{-1} band which corresponds to the ethylenic CH bond transitions, one can observe three main absorptions because of a Fermi resonance between the CH bond stretches and the overtone of HCH bending. For all the transitions, the μ_x component is very weak. The higher band at 2943 cm^{-1} has essentially a μ_y component and thus a PR envelope. When the molecule is bent, its energy comes essentially from the equatorial bond stretch. In the plane conformation, it corresponds to the CH_2 bend overtone which draws its energy from the symmetric stretch. The lower absorption at 2861 cm^{-1} has a more pronounced axial character for the transitions corresponding to the bent molecule and thus a B−C hybrid type with a Q branch. When the molecule is in the plane conformation, it corresponds to the symmetric stretch and then has no μ_z component. Thus the transitions issued from levels above the barrier have only a PR envelope. The band at 2910 cm^{-1} corresponds to an antisymmetric mode with essentially a μ_z component. It has a C type profile with a sharp Q branch. The transitions issued from the levels above the barrier give rise to the second Q branch at 2913 cm^{-1}. The calculated spectrum reproduces reasonably well the experimental one. All three modes can be called dynamically normal modes because the vibrational energy variation is symmetric. The vibrational energy flows symmetrically from one bond to the another during the motion. By contrast, the dynamically local mode of the monohydrogenated cyclopentene CH bond stretching has an asymmetrical variation because it oscillates between the two axial and equatorial energies.

2. First Overtone. The first overtone spectra of the two compounds have a more similar pattern to each other. The spectrum of the monohydrogenated cyclopentene is composed essentially of two bands at 5643 and 5740 cm^{-1} corresponding to the two axial and equatorial positions (Figure 2 of ref 17). The intermediate bands due to transitions issued from ring-puckering levels above the barrier are less intense than in the first excited spectrum because of the increase of the excited effective potential barrier height. In the spectrum of cyclopentene-d_4 (Figure 5), one can observe bands with the same contour at 5630 and 5728 cm^{-1}. They effectively correspond to the axial and equatorial transitions. The Fermi resonance is slightly detuned and the intermediate band is no more intense. However, the interactions between the CH stretches are still effective when the molecule is in the plane conformation and the vibrational energy variation shows a similar dynamically normal mode behavior as for the first excited spectrum. The strong absorption at 5815 cm^{-1} corresponds to the combination of the two CH stretching modes. In the calculated spectrum, an arbitrary value has been given to the second derivative $\partial^2\mu/\partial r_1\partial r_2$ ($\partial^2\bar{\mu}(x)/\partial r_1\partial r_2$

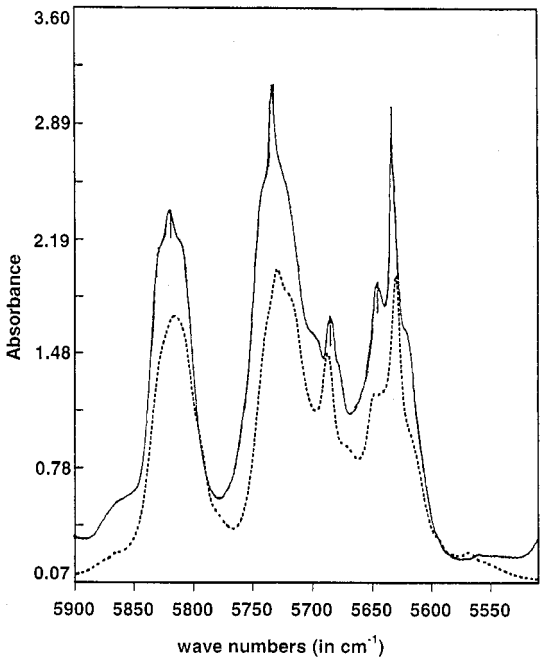

Figure 5. Observed and calculated spectra of the first overtone of the CH bond stretching in cyclopentene-d_4. The observed spectrum (top full line) was obtained by FTIR with a 1 m path length cell and a pressure of 200 Torr. The dashed line represents the calculated spectrum with a vibration−rotation theoretical profile which has been convoluted by a 9.5 cm^{-1} half-width Lorentzian band shape (fwhh).

$= (\partial^2\bar{\mu}(x)/\partial r_1^2 + \partial^2\bar{\mu}(x)/\partial r_2^2)/2)$ since this parameter is not avalaible for cyclopentene. Such a value leads to a correct reproduction of the observed spectrum. The real value is slightly lower than this arbitrary value in cyclopentene.

3. Second Overtone. The second overtone spectra of the two compounds (Figure 7) show small perturbations due to Fermi resonances. Indeed, on the low-frequency side of the two main bands corresponding to the axial (near 8280 cm^{-1}) and equatorial transitions (at 8430 cm^{-1} for cyclopentene-$3h_1$ and 8419 cm^{-1} for cyclopentene-d_4), one can observe one or two weak bands. In cyclopentene-$3h_1$, two kinds of mode begin to interact with the CH overtone: the HCD bending mode and the wagging mode. The diagonalization of the Hamiltonian matrix leads to three important vibrational energy variations $\omega_n(x)$ (Figure 6a); the first one gives the axial and equatorial transitions and the small bands around 8360 cm^{-1} which are the sum of the transitions issued from ring-puckering levels above the potential barrier. The two other $\omega_n(x)$ are responsible for the small absorptions on the low-frequency side. Although the spectrum of cyclopentene-d_4 seems very similar to that of monohydrogenated cyclopentene, the vibrational energy variations are different (Figure 6b). Two pairs of $\omega_n(x)$ have a local mode regime similar to that observed in the monohydrogenated compound. But because the two vibrational energy variations conserve the symmetric normal mode regime, each axial or equatorial band is composed of three components, two local and one normal. The small bands near 8350 cm^{-1} correspond to the transitions issued from ring-puckering levels above the potential barrier when the excited effective potential has a local vibrational variation. The lower pair of $\omega_n(x)$ gives the band at 8181 cm^{-1} which has an axial character since the equatorial transitions have no intensity for those effective potentials. The mixing of normal and local modes is a consequence of the onset of Fermi resonances with the combinations of HCH bending and HCC deformation modes.

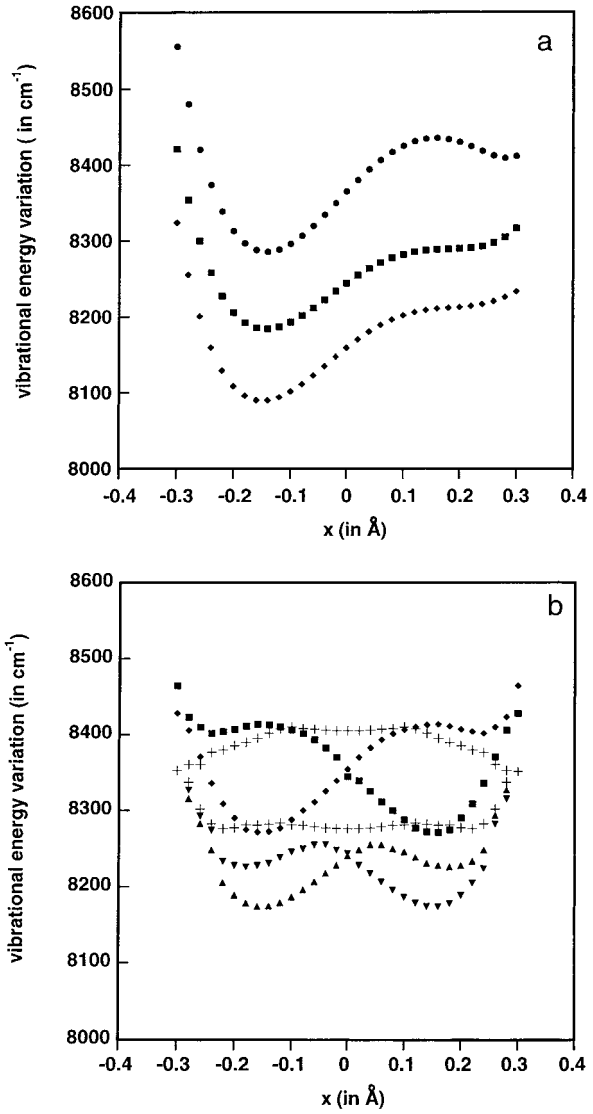

Figure 6. Calculated vibrational energy variations for cyclopentene-$3h_1$ (a) and cyclopentene-d_4 (b) at $\Delta v = 3$. The axial bent conformation corresponds to a value of $x = -0.13$ Å and the equatorial bent conformation to $x = 0.13$ Å. In Figure 6(b), + indicates a symmetric normal mode regime.

4. Third Overtone. The third overtone spectra of the two compounds are completely different (Figure 8): they are perturbed by Fermi resonances with combination states involving specific modes of the two cyclopentene molecules: HCD bending and HCC deformations for cyclopentene-$3h_1$ and wagging, and twisting modes for cyclopentene-d_4. For the reproduction of these modes, the diagonal force constants of ref 31 have been used. To validate the effective interactions between the angle deformations displayed in Table 3, the bending, wagging, and twisting mode wavenumbers of five cyclopentene isotopomers (cyclopentene-$3h_1$,-d_4,-h_8,-$4h_1$ (with only one CH bond on carbon 4), and cyclopentene-1,2,3,3-d_4 of ref 31) have been adjusted with the same effective interaction parameters. The results for cyclopentene-$3h_1$ and -d_4 are displayed in Table 4. Except for the HCD rock, which is not pure and does not enter in resonance with the CH bond stretch at the energies considered, there is a good concordance between observed and calculated deformation modes. In cyclopentene-$3h_1$, the combinations of three quanta in CH bond stretching and overtones of HCD bend or parallel HCC deformation split the CH stretch overtone into three main components which give

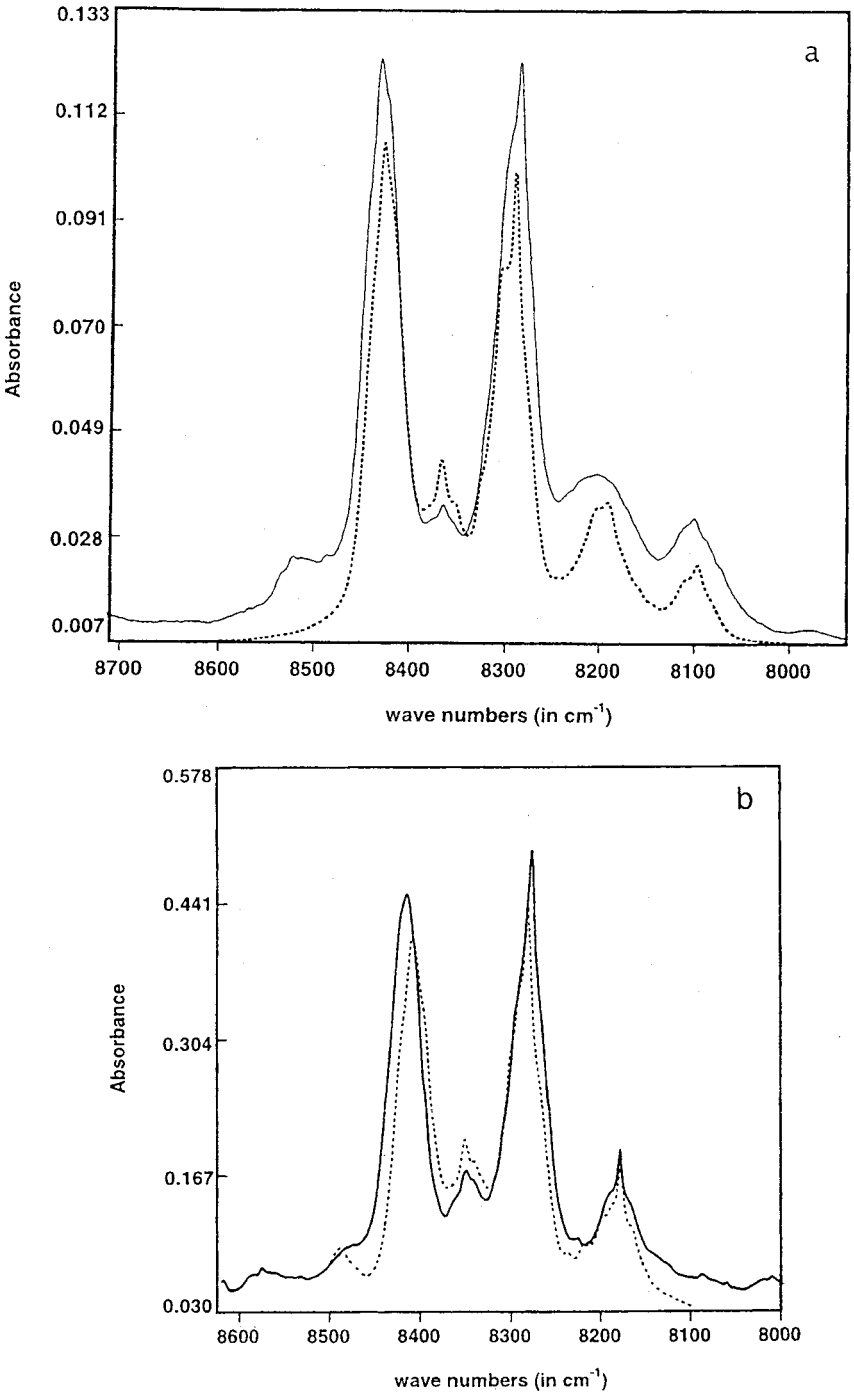

Figure 7. Observed and calculated spectra of the second overtone of the CH bond stretching in cyclopentene-$3h_1$ (a) and cyclopentene-d_4 (b). The observed spectra (top solid line) was obtained by FTIR with a 7 m path length cell and a pressure of 200 Torr for cyclopentene-d_4 and 90 Torr for cyclopentene-$3h_1$. The dotted lines represent the calculated spectrum with a vibration−rotation theoretical profile which has been convoluted by a 10 cm^{-1} half-width Lorentzian (fwhh).

rise to six bands (three axial and three equatorial transitions).The lower transition near 10 700 cm^{-1} and the shoulder near 10 800 cm^{-1} have an axial character. The stronger absorption near 10 870 cm^{-1} is the sum of two transitions, one axial and one equatorial. The upper part of the spectrum results from equatorial transitions. The variations of the vibrational energy for these three components are less important than would be the case without Fermi resonances. On the low energy side of the spectrum, there are also two weak axial transitions corresponding to combinations of two quanta of CH stretching and four quanta of angle deformations.

In the third overtone spectrum of cyclopentene-d_4, the axial and equatorial transitions are more separated. The calculated spectrum is the result of eight pairs of components with a local character. The calculated spectrum shows some discrepancies with the observed one, in particular in the axial region. This is partly due to a poor reproduction of the band shapes.

5. Fourth Overtone. The fourth overtone spectra of the two compounds are the least well reproduced (Figure 9). They have a more bulky shape than the lower excited spectra, which would indicate that they are formed of numerous bands. The diagonalization of the vibrational Hamiltonian leads to nine pairs of $\omega_n(x)$ with some intensity for the cyclopentene-d_4 molecule and six components in the case of cyclopentene-$3h_1$. The reproduc-

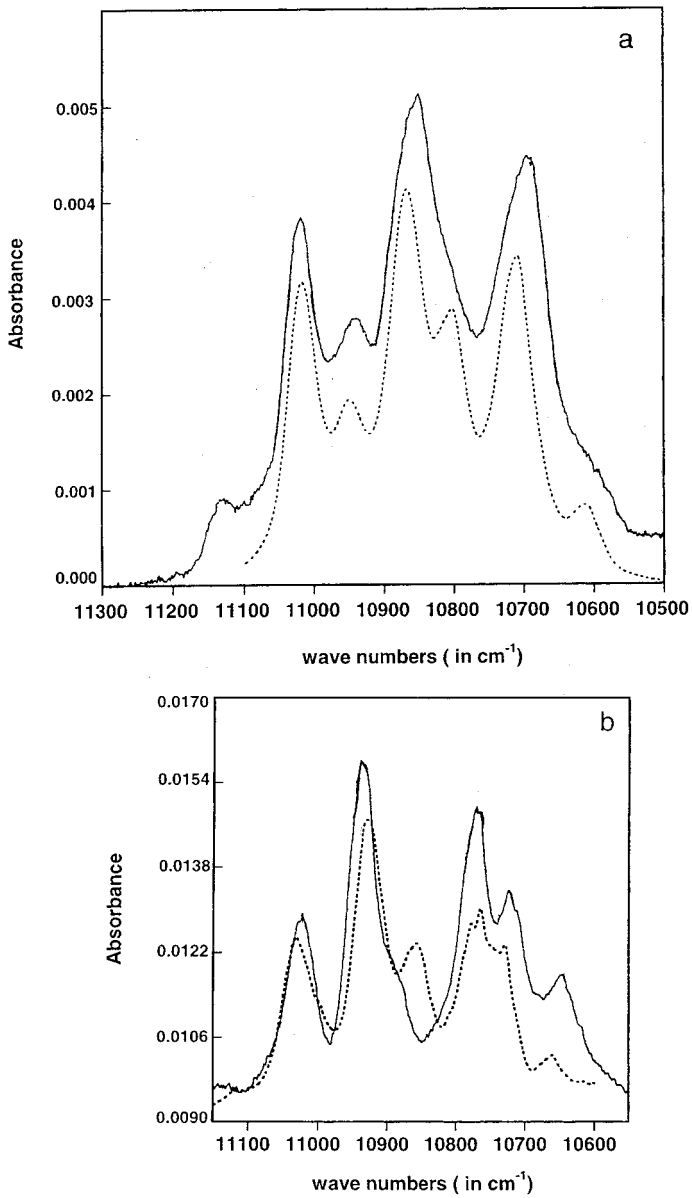

Figure 8. Observed and calculated spectra of the third overtone of the CH bond stretching in cyclopentene-$3h_1$ (a) and cyclopentene-d_4 (b). The observed spectra (top solid line) was obtained by FTIR with a 7 m path length cell and a pressure of 200 Torr. The dotted lines represent the calculated spectrum with a vibration−rotation theoretical profile which has been convoluted by a 25 cm^{-1} half-width Lorentzian (fwhh) for cyclopentene-$3h_1$ and 15 cm^{-1} for cyclopentene-d_4.

TABLE 4: Calculated and Observed Angle Deformation Modes (in cm^{-1})

	cyclopentene-d_4	
	calcd	obsd
HCH bend	1456	1456
wagging	1284	1284
twisting	1188	1188
rocking	1012	1013

	cyclopentene-$3h_1$ (axial)		cyclopentene-$3h_1$ (equatorial)	
	calcd	obsd	calcd	obsd
HCD bend	1303	1298	1306	1310
parallel HCC deformation	1245	1247	1252	1256
HCD rock	900	953	905	953

tion of the spectra shows that this is not sufficient, especially in the axial lower part. Something is missing in the vibrational Hamiltonian. At these energies, it would be the combinations of HCC deformations and CC stretches that could enter into resonance with the CH overtone. We have not introduced these modes for two reasons: (1) the ring modes are delocalized in the molecule and are not easily modeled inside the chromophore, and (2) the number of states would increase enormously and the diagonalization procedure we use would not afford such a number of states. In molecules such as cyclopentene, where there are many resonances, all the combination states have to be introduced in the calculations.

This coupling seems to affect essentially the axial transitions in cyclopentene-$3h_1$ and the equatorial transitions in the cyclopentene-d_4 molecule. It seems logical that these combination states, which have lower wavenumbers in cyclopentene-$3h_1$ affect modes at lower energies.

6. Fifth Overtone. The fifth overtone spectra are displayed in Figure 10. They show two main absorptions: one axial near 15 250 cm^{-1} and some equatorial bands above 15 600 cm^{-1}. The splitting of the equatorial bands is still visible in the spectra for each compound despite their bulky shape. The calculated

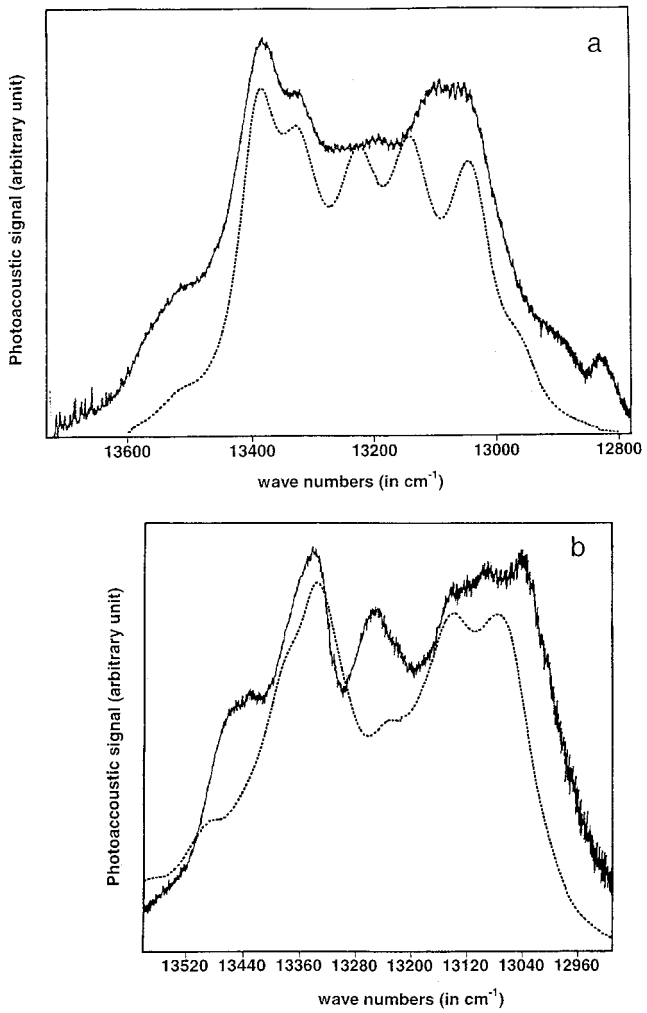

Figure 9. Observed and calculated spectra of the fourth overtone of the CH bond stretching in cyclopentene-3h$_1$ (a) and cyclopentene-d_4 (b). The observed spectra (top full line) was obtained by photoacoustic intracavity laser spectroscopy with a pressure of 200 Torr. The dotted lines represent the calculated spectrum with a vibration−rotation theoretical profile that has been convoluted by a 65 cm^{-1} half-width Lorentzian (fwhh) for cyclopentene-3h$_1$ and 45 cm^{-1} for cyclopentene-d_4.

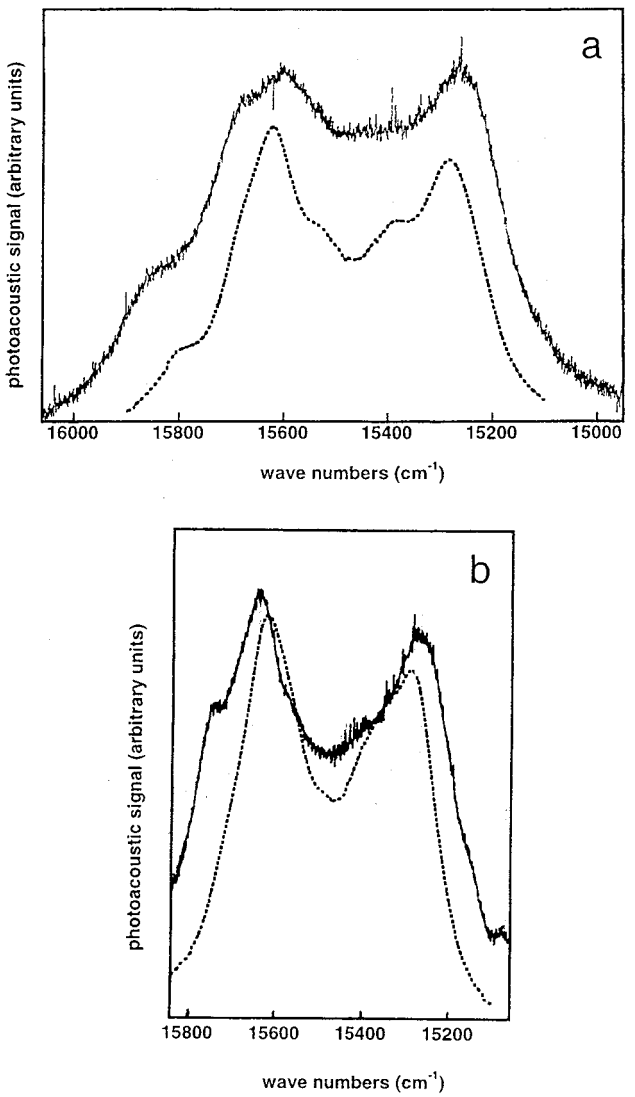

Figure 10. Observed and calculated spectra of the fifth overtone of the CH bond stretching in cyclopentene-3h$_1$ (a) and cyclopentene-d_4 (b). The observed spectra (top solid line) was obtained by photoacoustic intracavity laser spectroscopy with a pressure of 200 Torr. The dashed dotted lines represent the calculated spectrum with a vibration−rotation theoretical profile that has been convoluted by a 95 cm^{-1} half-width Lorentzian (fwhh) for cyclopentene-3h$_1$ and 65 cm^{-1} for cyclopentene-d_4.

spectrum of the cyclopentene-3h$_1$ molecule is the resultant of nine main components. But they generally give rise to only one band with some intensity, either axial or equatorial. There is only one $\omega_n(x)$ at intermediate energy, which gives rise to two shoulders in the medium of the spectrum. The vibrational energy variation of all the components would give an energy difference of 200 cm^{-1} between the axial and the equatorial transitions if observed. This is much less than the energy difference of more than 300 cm^{-1} between the two main absorptions of the observed spectra. The variation of the CH bond stretch not perturbed by Fermi resonance would also lead to an energy difference of 330 cm^{-1} between the axial and the equatorial main transitions. The couplings between the CH bond stretching overtones and the combination modes involving the angle deformations have the effect of drastically decreasing the vibrational energy variations during the motion.

This phenomenon is also observed in the cyclopentene-d_4 molecule. The $\Delta v = 6$ spectrum has some similarities with that of cyclopentene-3h$_1$. The main axial transitions are approximately at the same wavenumber. The equatorial bands of cyclopentene-d_4 are slightly higher than that of cyclopentene-3h$_1$. There are fewer transitions in the medium. The calculated spectrum is the sum of 22 bands. For the cyclopentene-d_4 compound, the couplings with the chromophore angle states split the CH stretching overtone into a great number of components which has the effect of essentially increasing the bandwidth. The statistical limit is almost reached.

In Table 5 the main Fermi resonance couplings and cross anharmonicities resulting from the anharmonic potentials of Table 3 are displayed. The former are defined as the $d_{r_i\alpha_j\alpha_k}$ of ref 32. They have the same order of magnitude as the methyle parameters of nitromethane[12] when the CH bond is perpendicular to the NO_2 plane. In the cyclopentene molecule, there are generally small variations of the parameters between the two axial and equatorial positions. It is apparent that the main Fermi resonance couplings concerning the HCC deformations are slightly more important than the bending ones. This is in agreement with the normal mode parameters.[7] On the contrary, the cross anharmonicities are relatively different in the two approaches: they strongly depend on the unperturbed wavenumber of the deformation mode. It must be stressed that it is

TABLE 5: Resultant Fermi Resonance Couplings $\lambda_{r\theta_i\theta_j}$ for Cyclopentene-d_4 (in cm^{-1}) and Cyclopentene-3h$_1$

θ_j/θ_i	δ	w$_1$	w$_2$	w$_3$	w$_4$
with respect to the first axial CH bond					
δ	15.0	−2.6	−2.6	3.9	3.9
w_1	−2.6	22.1	−8.1	11.9	0.0
w_2	−2.6	−8.1	22.1	0.0	11.9
w_3	3.9	11.9	0.0	9.5	0.0
w_4	3.9	0.0	11.9	0.0	9.5
with respect to the same CH bond but in equatorial position					
δ	16.8	2.3	2.3	−3.1	−3.1
w_1	2.3	21.1	−15.0	11.8	0.0
w_2	2.3	−15.0	21.1	0.0	11.8
w_3	−3.1	11.8	0.0	3.8	0.
w_4	−3.1	0.0	11.8	0.0	3.8
for cyclopentene-3h$_1$ with respect to the axial CH bond					
δ	18.7	−6.1	−6.1	5.2	5.2
w$_1$	−6.1	22.1	−8.1	12.9	0.0
w$_2$	−6.1	−8.1	22.1	0.0	12.9
w$_3$	5.2	12.9	0.0	9.3	0.0
w$_4$	5.2	0.0	12.9	0.0	9.3
for cyclopentene-3h$_1$ with respect to the same CH bond but in equatorial conformation					
δ	20.2	−1.3	−1.3	−0.6	−0.6
w$_1$	−1.3	21.1	−15.0	12.9	0.0
w$_2$	−1.3	−15.0	21.1	0.0	12.9
w$_3$	−0.6	12.9	0.0	3.1	0.0
w$_4$	−0.6	0.0	12.8	0.0	3.1
resultant cross anharmonicities					
for cyclopentene-3h$_1$ in axial and equatorial conformations:					
with the bending δ: −20.5 cm^{-1}					
with the HCC deformations adjacent to the CH bond:					
12 cm^{-1} (axial) and 13 cm^{-1} (equatorial)					
for cyclopentene-d_4:					
with the bending δ: −21 cm^{-1}					
with the HCC deformations adjacent to the CH bond:					
12 cm^{-1} (axial) and 13 cm^{-1} (equatorial)					

difficult to optimize all the model parameters simultaneously and the solution displayed here may not be unique. For this reason, it is of interest to test the solution on two isotopomers of the same molecule. In the present work, the uncertainties of the parameters certainly come essentially from the neglect of the coupling of the CH bond stretches with the combinations of CC stretches and HCC deformations.

V. Conclusion

The experimental spectra of two isotopomers of the cyclopentene molecule have been measured and analyzed with a theoretical treatment that takes into account the coupling between the CH bond stretches and the large amplitude ring-puckering motion within the adiabatic approximation. In the cyclopentene-d_4 molecule, this model clearly evidences the progressive dynamical localization of the vibrational energy. The signature of the dynamical localization is the presence of transitions at wavenumbers intermediate between the axial and equatorial bands if the barrier height of the excited effective ring-puckering potential is not too high. In the first excited spectrum, there is no evidence of such transitions but instead one can observe, for the intermediate band, a doubling of the sharp Q branch indicative of transitions issued from ring-puckering levels above the potential well in the vicinity of the transitions issued from levels in the bottom of the potential wells. This indicates that the effective excited potential is not very different from the fundamental potential and thus, the vibrational energy variation during the motion conserves a normal mode regime. The vibrational energy localization appears at the second overtone. At this energy, the spectra of the two compounds are very similar. Up to $\Delta v = 3$, the modeled spectra within the adiabatic approximation reproduce in a good manner the features of the experimental spectra.

At higher energies, the overtone spectra also show evidence of a rapid energy flow due to anharmonic couplings with isoenergetic combination states. They have been modeled in the framework of the HCH or HCD chromophore, ignoring in a first step the possible couplings involving the CC stretching modes, with a simple vibrational Hamiltonian written in internal curvilinear coordinates in order to reproduce the spectra of the two compounds with the same anharmonic potential. Even with these approximations, the general features of the spectra of the two isotopomers are reproduced. However, from the $\Delta v = 5$ overtone, some intensity transitions are not very well reproduced, indicating that other couplings are efficient at these energies. They possibly involve combinations of HCC deformations and CC stretching. In fact, the first derivative with respect to the CH bond stretch of the $g_{r_{CC}}\alpha^0$ term leads to a nonnegligible anharmonic coupling term. The CC bond stretches are delocalized into ring modes[33] from 1037 to 600 cm^{-1}. The combinations of the wagging and the first ring mode would have sufficient energy to interact with the higher CH bond stretching overtones by both kinetic and potential anharmonic terms. Even if the coupling is weak (because of the delocalization of the ring mode), it can modify somewhat the transition intensities. Further work is in progress in this field.

The comparison of the modeling of the cyclopentene-3h$_1$ overtone spectra in normal coordinates[7] with the present work indicates that the use of internal coordinates, with more constraints, conducts to essentially the same reproduction of the spectra as the other procedure, since, in this paper, the overtone spectra of two isotopic compounds have been fitted with the same anharmonic potential. The reproduction of the second and third overtones are almost equivalent in the two procedures. In the present study, the wavenumbers of the axial transitions in the third overtone are a little too high but the equatorial band at 10 955 cm^{-1} is better reproduced than in ref 7. For the fourth overtone, the axial transitons are not very well reproduced in the two procedures. The fifth overtone is slightly better in the present work since the transition near 15 500 cm^{-1} is less intense, and this corresponds better to the spectra. Furthermore, the conclusion of ref 7 was the same as the present one since the introduction of a ring mode weakly coupled with the twisting improved the higher overtone spectra ($\Delta = 6$ or 7). As a conclusion, the description of the rapid vibrational energy flow in internal coordinates can give good results in the frame of the methylene chromophore even in a relatively complex molecule such as cyclopentene. Its only disavantage is that it introduces a greater number of states in the fitting procedure.

Acknowledgment. We are grateful to J. C. Cornut and J. J. Martin for assistance in the experiments. We acknowledge support of this research by the Region Aquitaine through the award of equipment grants.

References and Notes

(1) Nesbitt, D. J.; Field, R. W. *J. Phys. Chem.* **1996**, *100*, 12 735.
(2) Quack, M. *Annu. Rev. Phys. Chem.* **1990**, *41*, 839.
(3) Crim, F. F. *Annu. Rev. Phys. Chem.* **1984**, *35*, 657.
(4) Dübal, H. R.; Quack, M. *J. Chem. Phys.* **1984**, *81*, 3779.
(5) Iung, C.; Leforestier, C. *J. Chem. Phys.* **1992**, *97*, 2481.
(6) Lespade, L.; Rodin, S.; Cavagnat, D.; Abbate S. *J. Phys. Chem.* **1993**, *97*, 6134.
(7) Rodin-Bercion, S.; Cavagnat, D.; Lespade, L.; Maraval, P. *J. Phys. Chem.* **1995**, *99*, 3005.

(8) Lespade, L.; Rodin-Bercion, S.; Cavagnat, D. *J. Phys. Chem.* **1997**, *101*, 2568.
(9) Henry, B. R.; Gough, K. M.; Sowa, M. G. *Int. Rev. Phys. Chem.* **1986**, *5*, 133.
(10) Cavagnat, D.; Cavagnat, R.; Cornut J. C.; Banisaed-Vahedie, S. *J. Phys.* **1992**, *C4*, 5205.
(11) Lehman, K. K.; Pates, B. H.; Scoles, G. *Annu. Rev. Phys. Chem.* **1994**, *45*, 241.
(12) Cavagnat, D.; Lespade, L.; Lapouge, C. *J. Chem. Phys.* **1995**, *103*, 10 502; Cavagnat, D.; and Lespade, L. *J. Chem. Phys.* **1998**, *108*, 9275.
(13) Cavagnat, D.; Lespade, L. *J. Chem. Phys.* **1997**, *106*, 7946.
(14) Cavagnat, D.; Banisaed-Vahedie, S.; Grignon-Dubois, M. *J. Phys. Chem.* **1991**, *99*, 5073.
(15) Lespade, L.; Rodin, S.; Cavagnat, D.; Abbate, S. *J. Phys. Colloq. 1* **1991**, *C7*, 517.
(16) Venuti, E.; Halonen, L.; Della Valle, R. G. *J. Chem. Phys.* **1999**, *110*, 7339.
(17) Lapouge, C.; Cavagnat, D.; Gorse, D.; Pesquer, M. *J. Phys. Chem.* **1995**, *99*, 2996; Lapouge, C. Ph.D. Thesis, University of Bordeaux I, 1996.
(18) Rodin-Bercion, S. Ph.D. Thesis, University of Bordeaux, 1993.
(19) Malloy, T. B. J. *Mol. Spectroscopy* **1972**, *44*, 504.
(20) Biarge, J. F.; Herrantz, J.; Morcillo, J. *J. Annu. Rev. Soc. Esp. Fis. Quim.* **1961**, *A57*.
(21) Person, W. B.; Newton, J. H. *J. Chem. Phys*. **1974**, *61*, 1040.
(22) Frisch, M. J.; Head-Gordon, M.; Schlegel, H. B.; Raghavachari, K.; Binkley, J. S.; Gonzalez, C.; Defrees, D. J.; Fox, D. J.; Whiteside, R. A.; Seeger, R.; Melius, C. F.; Baker, J.; Martin, R.; Kahn, L. R.; Steward, J. J. P.; Fluder, E. M.; Topiol, S.; Pople, J. A. Gaussian Inc., Pittsburgh, PA, 1988.
(23) Gough, K. M.; Murphy, W. F. *J. Chem. Phys.* **1987**, *87*, 1509.
(24) Podolsky, B. *Phys. Rev.* **1928**, *32*, 812.
(25) Meyer, R.; Günthard, Hs. H. *J. Chem. Phys.* **1968**, *49*, 1510; Pickett, H. M. *J. Chem. Phys.* **1972**, *56*, 1715.
(26) Wang, X. G.; Sibert, E. L., III. *J. Chem. Phys.* **1999**, *111*, 4510.
(27) Wallace, R. *Chem. Phys.* **1975**, *31*, 189; Sibert, E. L., III; Hynes, J. T.; Reinhardt, W. P. *J. Chem. Phys.* **1984**, *81*, 1115.
(28) Child, M. S.; Halonen, L. *Adv. Chem. Phys*. **1985**, *57*, 1.
(29) Halonen, L.; Carrington, T. C. *J. Chem. Phys*. **1988**, *88*, 4171.
(30) Leicknam, J. C. *Phys. Rev. A* **1980**, *22*, 2286.
(31) Villarreal, J. R.; Laane, J.; Bush, S. F.; Harris, W. C. *Spectrochim. Acta, Part A* **1979**, *35*, 331.
(32) Halonen, L. *J. Chem. Phys*. **1997**, *106*, 7931.
(33) Allen, W. D.; Csaszar, A. G.; Horner, D. A. *J. Am. Chem. Soc*. **1992**, *114*, 6834.